

Kinetics of Ligand Exchange in Rhodium-(I) and -(III) Complexes from Magnetisation-transfer Measurements; the Crystal Structure of $[\text{Rh}(\text{NH}_3)(\text{PPh}_3)_3]\text{ClO}_4^\dagger$

Lars A. Bengtsson,^{*a} Brian T. Heaton,^{*b} Jonathan A. Iggo,^b Chacko Jacob,^b Gary L. Monks,^b Jayakauri Ratnam^b and Anthony K. Smith^b

^a Department of Inorganic Chemistry 1, Chemical Centre, University of Lund, PO Box 124, S-221 00 Lund, Sweden

^b Department of Chemistry, Donnan Laboratories, University of Liverpool, PO Box 147, Liverpool L69 3BX, UK

Results from magnetisation-transfer measurements on $[\text{RhCl}(\text{PPh}_3)_3]$ and $[\text{RhH}_2\text{Cl}(\text{PPh}_3)_3]$ have been compared with data for analogous complexes obtained by replacing Cl with ONO_2 and NH_3 . For the chloro- and ammine-rhodium(I) complexes the rate constants for phosphine isomerisation and overall phosphine dissociation are similar and much lower than those observed for the nitrate complex. Nitrogen-15 NMR measurements show that this difference is probably due to the greater substitution lability of ONO_2 over Cl and NH_3 . For the rhodium(III) complexes it was possible to obtain rate constants for phosphine dissociation for both PPh_3 *trans* to PPh_3 and PPh_3 *trans* to H and similar rate constants are found for $[\text{RhH}_2\text{Cl}(\text{PPh}_3)_3]$ and $[\text{RhH}_2(\text{ONO}_2)(\text{PPh}_3)_3]$. These are larger than those for $[\text{RhH}_2(\text{NH}_3)(\text{PPh}_3)_3]\text{ClO}_4$, and this is consistent with going from a neutral to a cationic complex. In all three cases the rate constant for the fastest phosphine dissociation (*trans* to H) mirrors the rate of hydride isomerisation. The crystal structure of $[\text{Rh}(\text{NH}_3)(\text{PPh}_3)_3]\text{ClO}_4$ has been determined and the structural data are compared with those of other square-planar rhodium(I) complexes.

In the mid 1960s Wilkinson and co-workers¹ discovered that $[\text{RhCl}(\text{PPh}_3)_3]$ **1a** was an efficient catalyst for the hydrogenation of alkenes. Since then much work on the catalytic mechanism has been reported² and that proposed by Halpern³ is most generally accepted, although it should be pointed out that both spectroscopic characterisation and identification of the stereochemistry of many of the intermediates involved in the catalytic cycle is still lacking because such species are never found in sufficient concentrations to be detectable. The nature of these very active species has generally been inferred from analogies with more stable iridium species or complexes containing non-dissociating ligands.⁴ More recently, following Weitekamp's original experiments⁵ with *para*- H_2 , Eisenberg and co-workers⁶ have exploited the use of *para*- H_2 to confirm the reversible addition of H_2 to **1a** and Brown *et al.*⁷ have used spin-saturation-transfer measurements to obtain rate constants for PPh_3 exchange in both **1a** and $[\text{RhH}_2\text{Cl}(\text{PPh}_3)_3]$ **2a** as well as to obtain isomerisation rate constants between the inequivalent phosphine ligands in **1a** and between the inequivalent hydride ligands in **2a**.

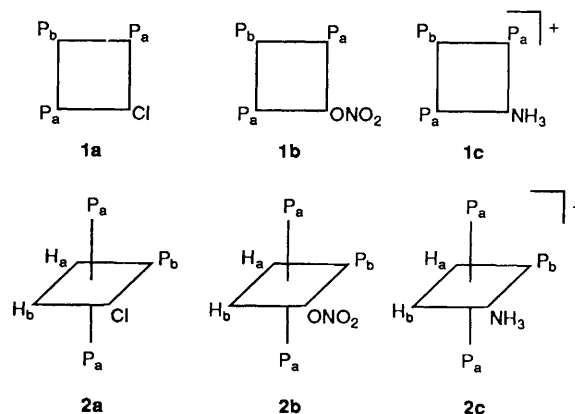
It was of interest to extend these measurements to other analogous complexes in order to investigate the effect of varying X in $[\text{RhX}(\text{PPh}_3)_3]^{n+}$ ($n = 0$, X = Cl **1a** or ONO_2 **1b**; $n = 1$, X = NH_3 **1c**) and $[\text{RhH}_2\text{X}(\text{PPh}_3)_3]^{n+}$ ($n = 0$, X = Cl **2a** or ONO_2 **2b**; $n = 1$, X = NH_3 **2c**). We now report a comparative spin-saturation-transfer study of these chloro, nitrate and ammine analogues of Rh^{I} and Rh^{III} together with ^{15}N NMR measurements in order to elucidate the rate of nitrate dissociation.

Structural data on complexes **1a**² and **1b**⁸ are available and for completeness we have also determined the crystal structure

of the perchlorate salt of **1c**. Structural data in the solid state on $[\text{RhH}_2\text{X}(\text{PPh}_3)_3]^{n+}$ ($n = 0$, X = Cl or ONO_2 ; $n = 1$, X = NH_3) are lacking because of the difficulty of obtaining X-ray-quality crystals. Nevertheless, the stereochemistry of all of these complexes is readily established from multinuclear NMR experiments in solution (see Experimental section).

Experimental

Materials and Solvents.—All preparations and manipulations of rhodium(I) compounds, **1a–1c** (see below), were routinely carried out under a nitrogen atmosphere except for the preparation of the rhodium(III) complexes **2a–2c** which involved bubbling H_2 through a solution of the rhodium(I) complex. The NMR data for **1a–1c** and **2a–2c** are given in Table 1; all NMR



[†] Supplementary data available: see Instructions for Authors, *J. Chem. Soc., Dalton Trans.*, 1994, Issue 1, pp. xxiii–xxviii.

measurements on complexes **2a–2c** were carried out under an atmosphere of H₂.

The solvent CD₂Cl₂ was obtained from Goss and dried over molecular sieves (4 Å) prior to use in the NMR measurements, all other solvents were dried using standard procedures. Sodium nitrate (99% ¹⁵N) was obtained from Merck Sharp & Dohme and used directly.

Preparations.—Methods described in the literature were used to prepare complexes **1a**¹ and **1b**.⁸

[Rh(NH₃)(PPh₃)₃]ClO₄. To a solution of RhCl₃·3H₂O (100 mg, 0.379 mmol) in methanol (6 cm³) was added solid AgClO₄ (235 mg, 1.133 mmol). The white precipitate of AgCl produced was allowed to settle overnight, filtered off and to the resulting orange solution was added a methanol solution (30 cm³) containing an excess of PPh₃ (600 mg, 2.3 mmol) and NH₄F (100 mg, 2.7 mmol). This solution was refluxed for 30 min, allowed to cool and on storing in a refrigerator (3 d) orange crystals of the pure product (yield 45%) were obtained as shown by ³¹P NMR spectroscopy and X-ray crystallography (Found: C, 63.65; H, 4.90; N, 1.05. Calc. for C₅₄H₄₈ClNO₄P₃Rh·CH₃·OH: C, 63.60; H, 5.05; N, 1.35%).

[Rh(ONO₂)(PPh₃)₃] **1b** (ca. 50% ¹⁵N-enriched). A mixture of Rh(NO₃)₃·2H₂O (0.539 g, 1.66 mmol) and ¹⁵N-enriched (99%) NaNO₃ (0.428 g, 4.98 mmol) was dissolved in water (2 cm³) and stirred for 1 h. This solution was evaporated to dryness *in vacuo* and the ¹⁵N-enriched Rh(NO₃)₃ was extracted with acetone (10 cm³). Evaporation of this solution to dryness gave Rh(NO₃)₃ (46.8% ¹⁵N from mass spectrometric analysis) which was used, as described previously,⁸ for the preparation of **1b** with ¹⁵N enrichment.

NMR Experiments.—The ¹H, ¹⁵N, ³¹P and ³¹P-¹H NMR experiments were performed on Bruker WM200, AC200 and AMX400 instruments. Chemical shifts are referenced to external standards, SiMe₄, MeNO₂ and H₃PO₄ (85% in water) respectively. The spin-saturation-transfer studies on each compound were confined to one specific spectrometer in order to minimise instrumental and magnetic field effects. The probe temperature was calibrated using a copper-constantan thermocouple.

In the kinetic studies the magnetisation transfer from a selectively inverted peak was observed as a function of time. The selective excitation was executed using the DANTE pulse sequence,¹⁰ relaxation delay-(pulse - τ)_{N-1}-pulse-mixing time- $\frac{\pi}{2}$ non-selective pulse-free-induction decay, where the effect of the *N* pulses sums to a selective π pulse. The values of τ and *N* have to be optimised for each system and instrument in order to obtain good selectivity and excitation. By varying the length of the mixing delay a series of spectra can be recorded from which the chemical exchange data are evaluated. The ³¹P NMR experiments are extremely time-consuming because of the long relaxation delays which have to be used due to slow relaxation of ³¹P. There is a constant compromise between a reasonable collection time and stability *versus* a good signal-to-noise ratio.

The ³¹P NMR spectra were preferably recorded with proton

coupling, since no extra delays for the switching between different decoupling powers have to be introduced and effects from nuclear Overhauser effects (NOEs) are absent. The spectra of all complexes of Rh^I and Rh^{III} described in this paper consist of a doublet of doublets and a doublet of triplets from co-ordinated phosphines together with a singlet from a trace of free triphenylphosphine.⁷ Usually, a small peak from triphenylphosphine oxide also appears. The hydride peaks in the ¹H NMR spectra of the rhodium(III) complexes are easily detected at negative chemical shifts.

The concentration of the rhodium-(I) and -(III) complexes was kept at approximately 25 mmol dm⁻³ in all experiments. In order to suppress the dissociation/association path of the reaction, no additional triphenylphosphine was added in the isomerisation experiments. In order to get reasonable overall reaction rates [see equation (3)] in the dissociation experiments the ratio of free phosphine: complex was 10:1, except for **1b**, for which the exchange reaction is so fast even at 233 K that this ratio had to be reduced to 2:1.

Data Treatment.—The isomerisation and association/dissociation of phosphine in the rhodium(I) complexes and hydride isomerisation in the rhodium(III) complexes were all treated as a two-site exchange between a site A and B [equation (1)]. Assuming a direct proportionality between the observed



macroscopic magnetisation, M_Z^i , and the concentrations of the phosphines at sites A and B, the exchange can be formulated using the Bloch equation formalism (2) where $R_i = k_i +$

$$\frac{d}{dt} \begin{bmatrix} M_Z^A - M_Z^A(\infty) \\ M_Z^B - M_Z^B(\infty) \end{bmatrix} = \begin{pmatrix} -R_A & k_B \\ k_A & -R_B \end{pmatrix} \begin{bmatrix} M_Z^A - M_Z^A(\infty) \\ M_Z^B - M_Z^B(\infty) \end{bmatrix} \quad (2)$$

($1/T_1^i$) and $M_Z^i(\infty)$ is the equilibrium magnetisation of the phosphines at each site *i*.

Magnetisation-transfer experiments have been reviewed by Mann and others fairly recently.^{11,12} The evaluation of these differential equations calls for special attention. In the isomerisation processes the solution becomes simple, since $k_{iso} = k_A = k_B$ and $1/T_1^A = 1/T_1^B$ can be assumed. The results were obtained by a linear regression analysis of the dependence of the function $\ln\{[M_Z^A - M_Z^A(\infty)] \pm [M_Z^B - M_Z^B(\infty)]\}$ on the mixing time *t*.¹³

For the dissociation/association processes the situation is slightly more complicated. A general solution for equation (2) has been suggested by Grassi *et al.*¹⁴ and partial solutions are given by McConnell.¹⁵ Full analytical solutions are given by Led and Gesmar¹⁶ and by Rudin.¹⁷ Given the initial

Table 1 Proton and ³¹P NMR data for rhodium(I) **1a–1c** and rhodium(III) complexes **2a–2c**

Complex	<i>T</i> /K	Solvent	δ(P _a)	δ(P _b)	¹ <i>J</i> (Rh–P _a)	¹ <i>J</i> (Rh–P _b)	² <i>J</i> (P _a –P _b)	δ(H _a)	δ(H _b)	² <i>J</i> (P _b –H _b)	Ref.
1a	303	<i>a</i>	32.2	48.9	146	192	37.5				9
1b	243	<i>a</i>	33.2	53.8	148	187	40				8
1c	303	<i>a</i>	34.7	45.5	142	168	40				This work
2a	233	<i>b</i>	41.4	21.0	113	88	21	-16.5	-9.2	155	7
2b	250	<i>c</i>	35.7	20.7	117	89	18	-20.8	-9.4	159	8
2c	303	<i>a</i>	42.2	28.7	112	93	18	-16.5	-10.6	144	This work

δ values in ppm; *J* in Hz.

^a CH₂Cl₂. ^b C₆H₅CH₃. ^c CDCl₃.

conditions, the eigenvalues and eigenfunctions can be derived. An elegant solution is to be published by Morris¹⁸ using a reduced-magnetisation formalism. In our experiments the ³¹P population difference of the free phosphine (site A) was normally inverted and the magnetisation transfer to co-ordinated phosphines (site B) recorded. This means that k_A in equation (2) corresponds to $k_{\text{ass}}[\text{RhX}(\text{PPh}_3)_2]$, k_B to k_{diss} , A to $^*\text{PPh}_3$, and B to $[\text{RhX}(^*\text{PPh}_3)(\text{PPh}_3)_2]$ as in equations (3) and (4).

$$d[^*\text{PPh}_3]/dt = -k_{\text{ass}}[\text{RhX}(\text{PPh}_3)_2][^*\text{PPh}_3] - (1/T_1^A[^*\text{PPh}_3]) + k_{\text{diss}}[\text{RhX}(^*\text{PPh}_3)(\text{PPh}_3)_2] \quad (3)$$

$$d[\text{RhX}(^*\text{PPh}_3)(\text{PPh}_3)_2]/dt = k_{\text{ass}}[\text{RhX}(\text{PPh}_3)_2][^*\text{PPh}_3] - k_{\text{diss}}[\text{RhX}(^*\text{PPh}_3)(\text{PPh}_3)_2] - \{1/T_1^B[\text{RhX}(^*\text{PPh}_3)(\text{PPh}_3)_2]\} \quad (4)$$

However, for a large number of experiments of different types the routine approach is iteration. The personal computer version of the program GIT based on the GEAR integration subroutine was used to obtain the best reaction models, in terms of reaction and relaxation rate constants, that fit the experimental data of the different systems.¹⁹⁻²¹ At least two separate experiments were evaluated for each reaction studied and the final results presented are the mean values.

The results from the dissociation of both types of phosphines in the octahedral rhodium(III) complexes represent a three-site exchange problem [equation (5)] where C = free PPh₃,



D = PPh₃ *trans* to PPh₃ (P_a in 2), E = PPh₃ *trans* to H (P_b in 2), with the direct exchange between the two types of co-ordinated phosphines (P_a and P_b) being negligible. The results were obtained iteratively by solving equation (6).

$$\frac{d}{dt} \begin{bmatrix} M_Z^C - M_Z^C(\infty) \\ M_Z^D - M_Z^D(\infty) \\ M_Z^E - M_Z^E(\infty) \end{bmatrix} = \begin{bmatrix} -\left(k_C + k_E + \frac{1}{T_1^C}\right) & k_D & k_F \\ k_C & -\left(k_D + \frac{1}{T_1^D}\right) & 0 \\ k_- & 0 & -\left(k_F + \frac{1}{T_1^E}\right) \end{bmatrix} \begin{bmatrix} M_Z^C - M_Z^C(\infty) \\ M_Z^D - M_Z^D(\infty) \\ M_Z^E - M_Z^E(\infty) \end{bmatrix} \quad (6)$$

The overall precision and accuracy in the iteratively obtained rate constants was estimated to be about 20%. The relaxation rates observed in the rhodium(I) and -(III) systems differed slightly from system to system and also between different batches of preparation in each system. This effect is probably a consequence of the required compromise between collection time and stability *versus* a good signal-to-noise ratio, and also the experimental procedure not being an ideal one for the determination of accurate relaxation rates. Furthermore, different preparations of specific complexes had different amounts of paramagnetic impurities (e.g. Rh^{II}), which influence the relaxation rates. Typical ³¹P relaxation times obtained in the rhodium(I) systems were 2–4 s for co-ordinated and 5–10 s for free phosphine, while in the rhodium(III) systems the relaxation times were consistently longer, amounting to 15–20 s.

X-Ray Crystallography.—X-Ray diffraction data were recorded on a Rigaku AFC-6S diffractometer operating in the ω-

scan mode with graphite-monochromated Mo-Kα radiation (λ = 0.710 69 Å), following standard procedures.

Crystal data. $[\text{Rh}(\text{NH}_3)(\text{PPh}_3)_3]\text{ClO}_4 \cdot \text{MeOH}$, C₅₅H₅₂ClNO₅P₃Rh, $M = 1038.3$, yellow prism (0.5 × 0.25 × 0.5 mm) orthorhombic, space group *Aba2* (no. 41), $a = 25.42(1)$, $b = 18.52(2)$, $c = 21.41(1)$ Å, $U = 10\,079$ Å³, $Z = 8$, $D_c = 1.367$ g cm⁻³, $F(000) = 4280$, $\mu(\text{Mo-K}\alpha) = 5.26$ cm⁻¹.

4840 Reflections were recorded ($2\theta_{\text{max}} = 50^\circ$) of which 3025 with $I > 3.0\sigma(I)$ were used in the refinement. An empirical absorption correction (DIFABS)²² was applied (transmission factors 0.62–1.20). The structure was solved by direct methods (SHELX 86).²³ Full-matrix least-squares refinement converged to R and R' factors of 0.076 and 0.085 respectively and the weighting scheme was based on $(|F_o| - |F_c|)^2/|F_o|$; the Rh, N and P atoms were refined anisotropically with all other atoms refined isotropically. Atom coordinates are given in Table 4 with selected bond lengths and angles in Table 5. Refinement of the structure was hampered by the methanol present as solvent of crystallisation and a poorly refined perchlorate ion, which is disordered across a two-fold axis. The most satisfactory refinement was achieved with the perchlorate having half occupancy at two sites.

Additional material available from the Cambridge Crystallographic Data Centre comprises H-atom co-ordinates, thermal parameters and remaining bond lengths and angles.

Results and Discussion

The basic objective in this work was to investigate the rates of triphenylphosphine dissociation in a series of analogous complexes of Rh^I and Rh^{III} with different ligands X (= Cl, ONO₂ or NH₃), in order to obtain information regarding reaction mechanisms which may be important in obtaining a better understanding of their efficiency in catalytic hydrogenation. Phosphine-dissociation rate constants for $[\text{RhCl}(\text{PPh}_3)_3]$ have previously been reported by Halpern and Wong²⁴ using stopped-flow spectrophotometry and by Brown and co-workers^{7,25} using the magnetisation-transfer NMR technique.

These data on the dynamics of phosphine exchange in $[\text{RhCl}(\text{PPh}_3)_3]$ have been used as a reference point in the present investigation.

$[\text{RhX}(\text{PPh}_3)_3]^{n+}$ ($n = 0$, X = Cl or ONO₂; $n = 1$, X = NH₃).—A significant dynamic feature in all of these square-planar rhodium(I) complexes is the fast isomerisation (k_{iso}) between phosphines co-ordinated *cis* and *trans* to the ligand X. All three complexes give similar ³¹P magnetisation-transfer NMR spectra as a function of time. The experimental kinetic data for X = Cl, ONO₂ or NH₃, at 297, 233 and 303 K respectively, along with the iteratively obtained best fits by equation (2), are shown in Fig. 1(a)–1(c), respectively. These results, in terms of isomerisation rate constants, are summarised in Table 2. The isomerisation measurements were carried out in the absence of added triphenylphosphine in order to suppress the phosphine dissociation/association reaction path, whereas the dissociation measurements were made in the presence of free triphenylphosphine in order to get reasonable overall rates as

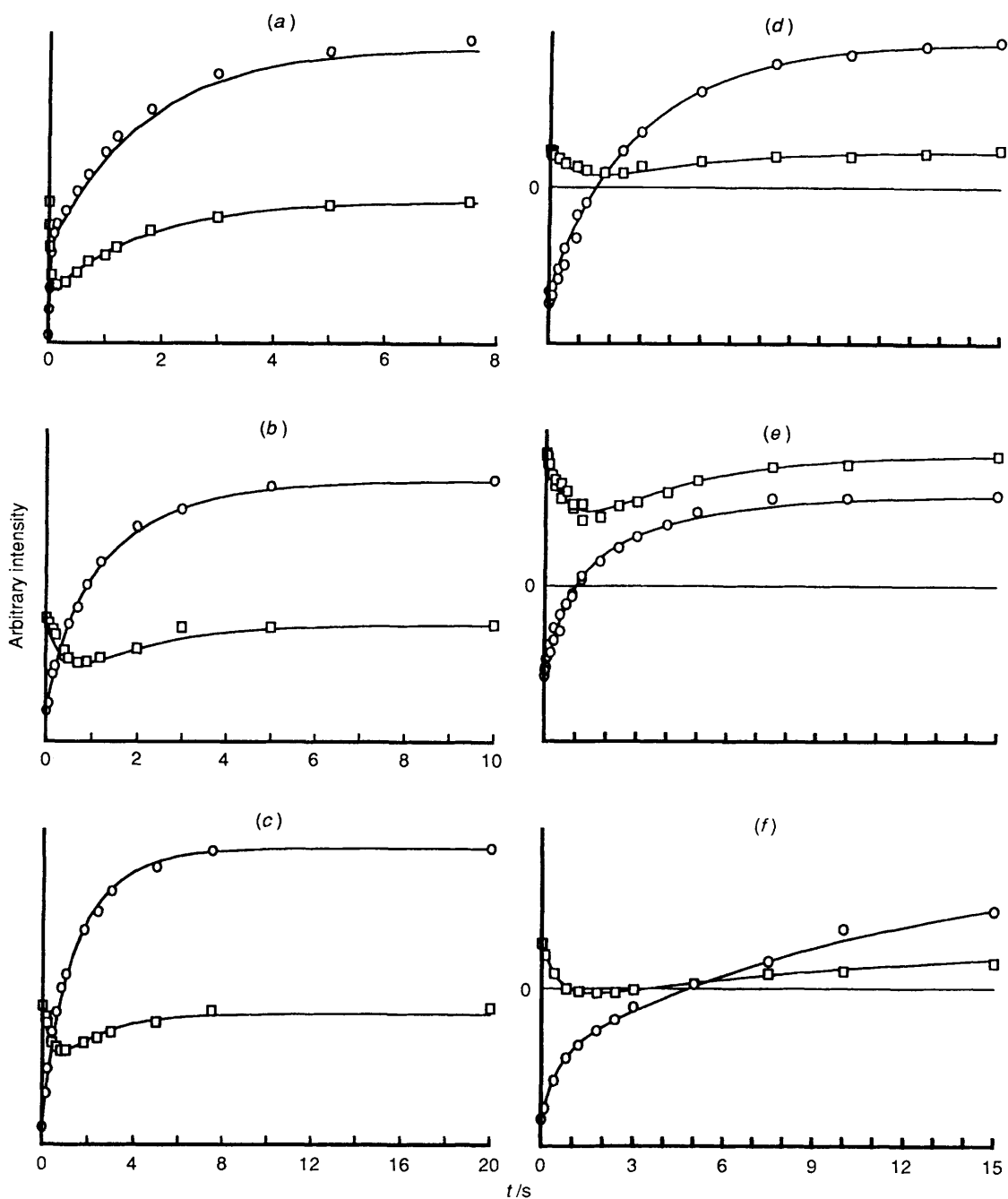


Fig. 1 (a)–(c) The isomerisation of triphenylphosphines P_a and P_b in complexes **1a**–**1c** respectively as monitored by magnetisation transfer. (○), Experimental intensities of the inverted doublet from P_a; (□), sum of the intensities of the two triplets from P_b. The full curves represent the best fit of the kinetic models [equation (2)]. (d)–(f) The overall dissociation of P_a/P_b in **1a**–**1c** respectively as monitored by magnetisation transfer. (○), Experimental intensities of the inverted free phosphine; (□), sum of the intensities of the doublet of doublets and triplets from co-ordinated P_a and P_b. Full curves as in (a)–(c)

described in the Experimental section. The phosphine-dissociation results are shown in Fig. 1(d)–1(f) and are summarised in Table 3.

It should be noted that both k_{iso} and k_{diss} are very much slower for the chloro and ammine than for the nitrate complex. For this reason the latter system had to be studied at a much lower temperature. The approximate rate constant at room temperature can be estimated by assuming the reaction rate constant increases by a factor of two for each increase of 10 °C. The result thus obtained coincides well with an estimate from the observed line broadening in the ^{31}P NMR spectrum at room temperature.

We have also measured the variable-temperature ^{15}N NMR spectrum of $^{15}\text{NO}_3$ -enriched (ca. 24%) complex **1b** [$\delta(^{15}\text{N}) = -12.8$ at 243 K] in the presence of an equimolar quantity of $^{15}\text{NO}_3$ -enriched (ca. 24%) NBu_4NO_3 [$\delta(^{15}\text{N}) = -2.9$ at 243 K] in CH_2Cl_2 . From the coalescence temperature on a Bruker AMX 400 spectrometer, the rate constant for nitrate dissociation at 303 K is $(2.7\text{--}4.3) \times 10^3 \text{ s}^{-1}$ which is significantly larger than the rate of phosphine isomerisation, k_{iso} .

Three possible simple mechanisms can be postulated for the isomerisation, the respective intermediates **3**–**5** being as shown in Scheme 1. In conjunction with the above rate of nitrate dissociation in complex **1b** and the well known leaving proper-

ties of nitrate in similar platinum(II) systems,²⁶ the involvement of **5** via the X-dissociative mechanism appears to be dominant for **1b** whereas involvement of the pseudo-tetrahedral intermediate **3** could be the dominant mechanism for the chloro and ammine complexes **1a** and **1c** as previously suggested by Brown and co-workers^{7,25} for **1a**. Although the magnetisation-transfer technique has also been used to study other rhodium systems^{27,28} and the dynamics of Rh^I and Rh^{III} has been briefly reviewed,²⁹⁻³¹ no detailed analysis of reaction mechanisms based on *cis/trans* influences, *cis/trans* effects or leaving-ligand effects seems to have been undertaken. Thus, literature analogies have to be sought on related systems like Pd^{II} and Pt^{II}.²⁶

The *cis/trans* effect and *cis/trans* influence of the phosphines are expected to be much larger than for any of the X ligands, and therefore the large dependence of the dissociation rate constant on X rules out any simple interaction between phosphines only. The dissociation rate constants are, as for the isomerisation rate constants, almost equal between the chloro and ammine complexes, but very much larger for the nitrate complex. The mechanism of phosphine exchange is most likely not a simple

Table 2 Rate constants for triphenylphosphine isomerisation in square-planar $[\text{RhX}(\text{PPh}_3)_3]^{n+}$ ($n = 0$, X = Cl or ONO_2 ; $n = 1$, X = NH_3) in CH_2Cl_2 solution

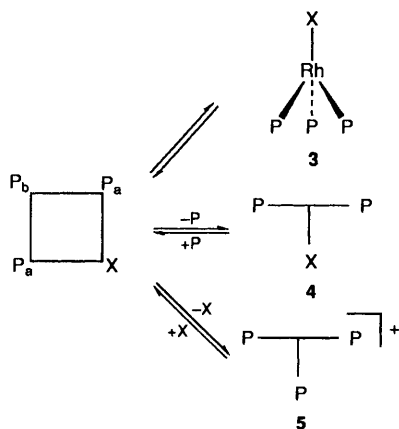
X	T/K	$k_{\text{iso}}^a/\text{s}^{-1}$	Relative k_{iso}^a	$k_{\text{iso}}^a/k_{\text{diss}}^b$
Cl	303	17	24	56.7
	297	11		
ONO_2	233	0.8		
	303 ^c	102	146	1.8
NH_3	303	0.7	1	0.5

^a k_{iso} is the rate of P_a/P_b isomerisation. ^b k_{diss} is the rate of overall P_a and P_b dissociation. ^c Data at 233 K extrapolated to 303 K as described in the text.

Table 3 Rate constants for triphenylphosphine dissociation in square-planar complexes $[\text{RhX}(\text{PPh}_3)_3]^{n+}$ ($n = 0$, X = Cl or ONO_2 ; $n = 1$, X = NH_3) in CH_2Cl_2 solution

X	T/K	$k_{\text{diss}}^a/\text{s}^{-1}$	Relative k_{diss}^a
Cl	303	0.3	1
ONO_2	233	0.5	
	303 ^b	58	193
NH_3	303	1.4	4.6

^a k_{diss} is the overall rate of P_a and P_b dissociation. ^b Data at 233 K extrapolated to 303 K as described in the text.



Scheme 1 P = PPh_3 , X = Cl, ONO_2 or NH_3

one, and clues to a plausible mechanism based on the special properties of nitrate as a leaving ligand can be obtained by comparison with the crystal structure and the temperature dependence of the ^{31}P NMR spectra of the T-shaped $[\text{Rh}(\text{PPh}_3)_3]^+$ cation.³² Consistent with the solid-state structure, the ^{31}P NMR spectrum of $[\text{Rh}(\text{PPh}_3)_3]\text{ClO}_4$ in CH_2Cl_2 solution at low temperature shows the presence of two resonances in the ratio 1:2 due to the unique and *trans*-phosphines respectively. When the temperature is increased, both resonances broaden and then coalesce to form a doublet. The preservation of $^1J(\text{Rh}-\text{P})$ at high temperatures is thus consistent with a fast intramolecular fluxional process for exchange of inequivalent triphenylphosphines. Addition of triphenylphosphine results in broadening of the NMR resonances and loss of $^1J(\text{Rh}-\text{P})$ consistent with the onset of intermolecular exchange processes but quantitative measurements of this system have not been carried out. This arises because of the instability of $[\text{Rh}(\text{PPh}_3)_3]\text{ClO}_4$ in CH_2Cl_2 solution over the time necessary to carry out the NMR measurements. The crystal structure of $[\text{Rh}(\text{PPh}_3)_3]\text{ClO}_4$ is also very interesting, since it shows how two of the phosphines co-operate to distort the third. Furthermore, there is no evidence in the solid state for either OClO_3 or CH_2Cl_2 , which was present as solvent of crystallisation, occupying the vacant co-ordination site of the rhodium(I) square plane in $[\text{Rh}(\text{PPh}_3)_3]^+$. It thus seems that **1b** undergoes a fast dissociation of nitrate to give the T-shaped complex $[\text{Rh}(\text{PPh}_3)_3]^+$, which then undergoes isomerisation and dissociation via the co-operative distortion discussed above.

Structure of $[\text{Rh}(\text{NH}_3)(\text{PPh}_3)_3]\text{ClO}_4$.—The perchlorate salt of the complex $[\text{Rh}(\text{NH}_3)(\text{PPh}_3)_3]^+$ **1c** crystallises as discrete $[\text{Rh}(\text{NH}_3)(\text{PPh}_3)_3]^+$ cations and perchlorate anions and contains one molecule of solvent of crystallisation (MeOH). In the cation (Fig. 2) the rhodium(I) is essentially square planar. In-plane deviations from ideal square-planar co-ordination consist of P–Rh–P angles greater than, and P–Rh–N angles less than, 90° as a result of the disparate steric differences between PPh_3 and NH_3 . The out-of-plane distortion towards tetrahedral co-ordination is very slight with NH_3 being most displaced; deviations of the atoms from the mean RhP_3N plane are Rh 0.010(1), P(1) $-0.087(4)$, P(2) $-0.098(5)$, P(3) 0.012(4) and N 0.251(14) Å.

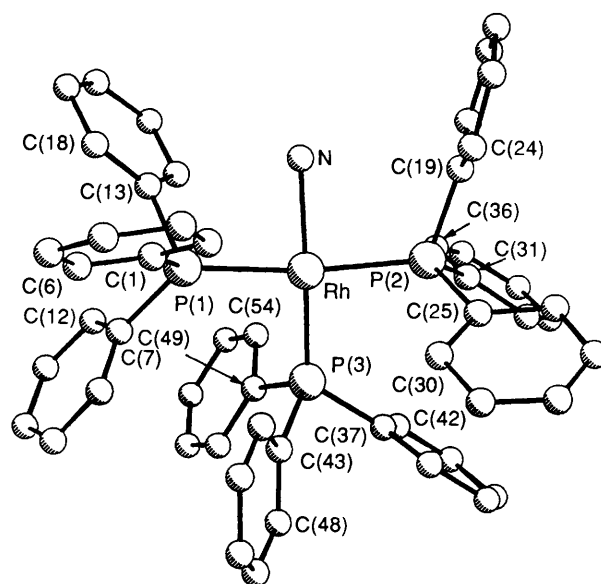
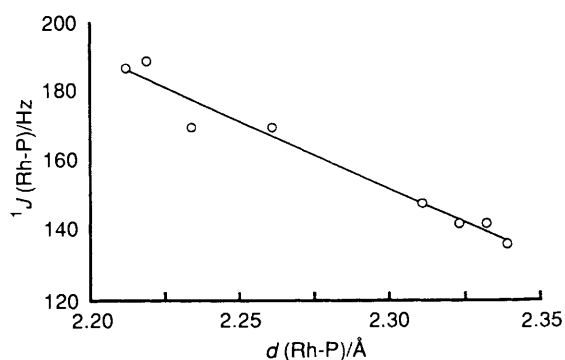


Fig. 2 Crystal structure of the cation of the square-planar complex $[\text{Rh}(\text{NH}_3)(\text{PPh}_3)_3]\text{ClO}_4 \cdot \text{MeOH}$

Table 4 Atomic coordinates for $[\text{Rh}(\text{NH}_3)(\text{PPh}_3)_3]\text{ClO}_4 \cdot \text{MeOH}$

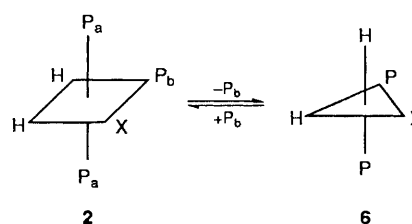
Atom	x	y	z	Atom	x	y	z
Rh	0.366 46(4)	0.756 46(6)	0.927 6	C(23)	0.385(1)	0.929(1)	1.124(1)
Cl(1)*	1	0	0.026 9(4)	C(24)	0.354 2(8)	0.888(1)	1.083 7(8)
Cl(2)*	0.5	0	0.008 4(6)	C(25)	0.261 2(7)	0.813 1(9)	1.021 2(8)
P(1)	0.414 7(2)	0.770 1(2)	0.835 3(2)	C(26)	0.232 3(8)	0.826(1)	1.076 0(8)
P(2)	0.323 6(2)	0.762 4(2)	1.022 9(2)	C(27)	0.183(1)	0.866(1)	1.070(1)
P(3)	0.305 4(1)	0.685 9(2)	0.883 3(2)	C(28)	0.168(1)	0.891(1)	1.016(1)
O(1)	1.025(1)	0.055(2)	-0.006(1)	C(29)	0.197(1)	0.881(1)	0.964(1)
O(2)	0.982(2)	0.029(2)	0.079(2)	C(30)	0.244 8(8)	0.844(1)	0.965 8(8)
O(3)	0.547(1)	0.025(2)	-0.016(1)	C(31)	0.311 0(7)	0.676(1)	1.063 2(8)
O(4)	0.476(2)	0.057(2)	0.045(2)	C(32)	0.262 0(8)	0.659(1)	1.091 1(8)
O(5)	0.011 0(9)	0.200(1)	0.047(1)	C(33)	0.259 9(9)	0.594(1)	1.123(1)
N	0.430 7(5)	0.813 0(7)	0.970 2(7)	C(34)	0.303(1)	0.548(1)	1.127(1)
C(1)	0.412 8(7)	0.862 3(9)	0.806 9(7)	C(35)	0.349(1)	0.563(1)	1.098(1)
C(2)	0.389 1(8)	0.914(1)	0.844 7(9)	C(36)	0.352 9(7)	0.625(1)	1.066 2(8)
C(3)	0.392(1)	0.987(1)	0.824(1)	C(37)	0.251 1(6)	0.639 9(7)	0.925 0(8)
C(4)	0.408(1)	1.004(1)	0.766(1)	C(38)	0.203 2(7)	0.676 0(9)	0.935(1)
C(5)	0.431(1)	0.955(1)	0.728(1)	C(39)	0.161 1(8)	0.641(1)	0.965 7(8)
C(6)	0.429 2(8)	0.884(1)	0.748 0(9)	C(40)	0.166 4(8)	0.573(1)	0.985 6(9)
C(7)	0.408 0(7)	0.719(1)	0.762 7(8)	C(41)	0.214 2(9)	0.536(1)	0.979(1)
C(8)	0.372 9(8)	0.736(1)	0.718 0(8)	C(42)	0.254 9(8)	0.572(1)	0.947 9(8)
C(9)	0.366 1(8)	0.697(1)	0.663 1(9)	C(43)	0.266 0(6)	0.731 4(9)	0.822 4(7)
C(10)	0.398(1)	0.640(1)	0.652(1)	C(44)	0.275 7(7)	0.804 8(9)	0.811 0(7)
C(11)	0.434 3(9)	0.618(1)	0.697(1)	C(45)	0.247(1)	0.842(1)	0.768(1)
C(12)	0.439 4(7)	0.656(1)	0.753 8(8)	C(46)	0.206 0(8)	0.805(1)	0.736(1)
C(13)	0.486 6(6)	0.756(1)	0.852 1(7)	C(47)	0.197 4(8)	0.736(1)	0.745(1)
C(14)	0.497 9(8)	0.697(1)	0.887 9(9)	C(48)	0.224 8(8)	0.694(1)	0.790(1)
C(15)	0.552(1)	0.678(1)	0.898(1)	C(49)	0.336 4(7)	0.607 1(9)	0.848 9(7)
C(16)	0.588 7(9)	0.725(1)	0.871(1)	C(50)	0.318 8(8)	0.570(1)	0.795 5(8)
C(17)	0.580(1)	0.783(1)	0.838(1)	C(51)	0.342 2(8)	0.506(1)	0.777 6(9)
C(18)	0.523 9(8)	0.800(1)	0.828(1)	C(52)	0.381 7(9)	0.479(1)	0.810(1)
C(19)	0.360 2(7)	0.813 3(8)	1.083 0(7)	C(53)	0.399 7(9)	0.513(1)	0.864(1)
C(20)	0.395 4(8)	0.781(1)	1.123(1)	C(54)	0.377 7(7)	0.575(1)	0.883 0(8)
C(21)	0.424 8(8)	0.824(1)	1.165(1)	C(55)	-0.036(1)	0.226(2)	0.075(1)
C(22)	0.422(1)	0.892(1)	1.163(1)				

* Site occupancy 0.5.

**Fig. 3** Comparison of selected Rh^I-P distances and $^1J(\text{Rh}-\text{P})$ in related square-planar complexes based on the data in Table 6

The values of $d(\text{Rh}-\text{P})$ for complex **1c** are summarised together with data for other analogues in Table 6 and it can be seen there is a close similarity in the distortions found for **1c** with those for $[\text{Rh}(\text{MeCN})(\text{PPh}_3)_3]\text{BF}_4$.³³ Table 6 shows that the Rh-P(3) bond length for all the complexes is shorter than $d[\text{Rh}-\text{P}(1)]$ and $d[\text{Rh}-\text{P}(2)]$ which show considerable variation. However, this is probably the result of packing effects since there is a very good relationship (Fig. 3) between the values of $^1J(\text{Rh}-\text{P})$ obtained in solution and both $d[\text{Rh}-\text{P}(3)]$ and the average of $d[\text{Rh}-\text{P}(1)]$ and $d[\text{Rh}-\text{P}(2)]$.

$[\text{RhH}_2\text{X}(\text{PPh}_3)_3]^{n+}$ ($n = 0$, X = Cl or ONO_2 ; $n = 1$, X = NH_3).—Experimental data on the dynamics of phosphine exchange in rhodium(III) complexes are also scarce, although

**Scheme 2**

from the presently available data there does appear to be a resemblance with the dynamics of analogous cobalt(III) complexes with the predominant mechanism of substitution being dissociative²⁹⁻³¹ (Scheme 2). No direct isomerisation between the equatorial (*trans* to H, P_b) and axial (*trans* to PPh_3 , P_a) phosphines seems to exist. In all complexes P_b exchanges with free phosphine at a much higher rate than does P_a (by a factor of 10–100). The hydride ligands are expected to have a very large *trans* influence, larger than phosphine, and the present experimental results thus agree with this prediction.²⁶ The results are given in Table 7 and Fig. 4(a)–4(c).

The dissociation rate constants are very much less dependent on the ligand X, and a more direct mechanism than indicated in the rhodium(I) systems may be dominant in all three cases. However, it should be noted that the phosphine-dissociation rate constants of the ammine complex are significantly lower than in the other systems, and may reflect the fact that the ammine complex is positively charged rather than neutral. We have also measured the ^{15}N NMR spectrum of ^{15}N -enriched (ca. 24%) **2b** [$\delta(^{15}\text{N}) -10.4$, $^2J(^{103}\text{Rh}-^{15}\text{N})$ 2 Hz] in the

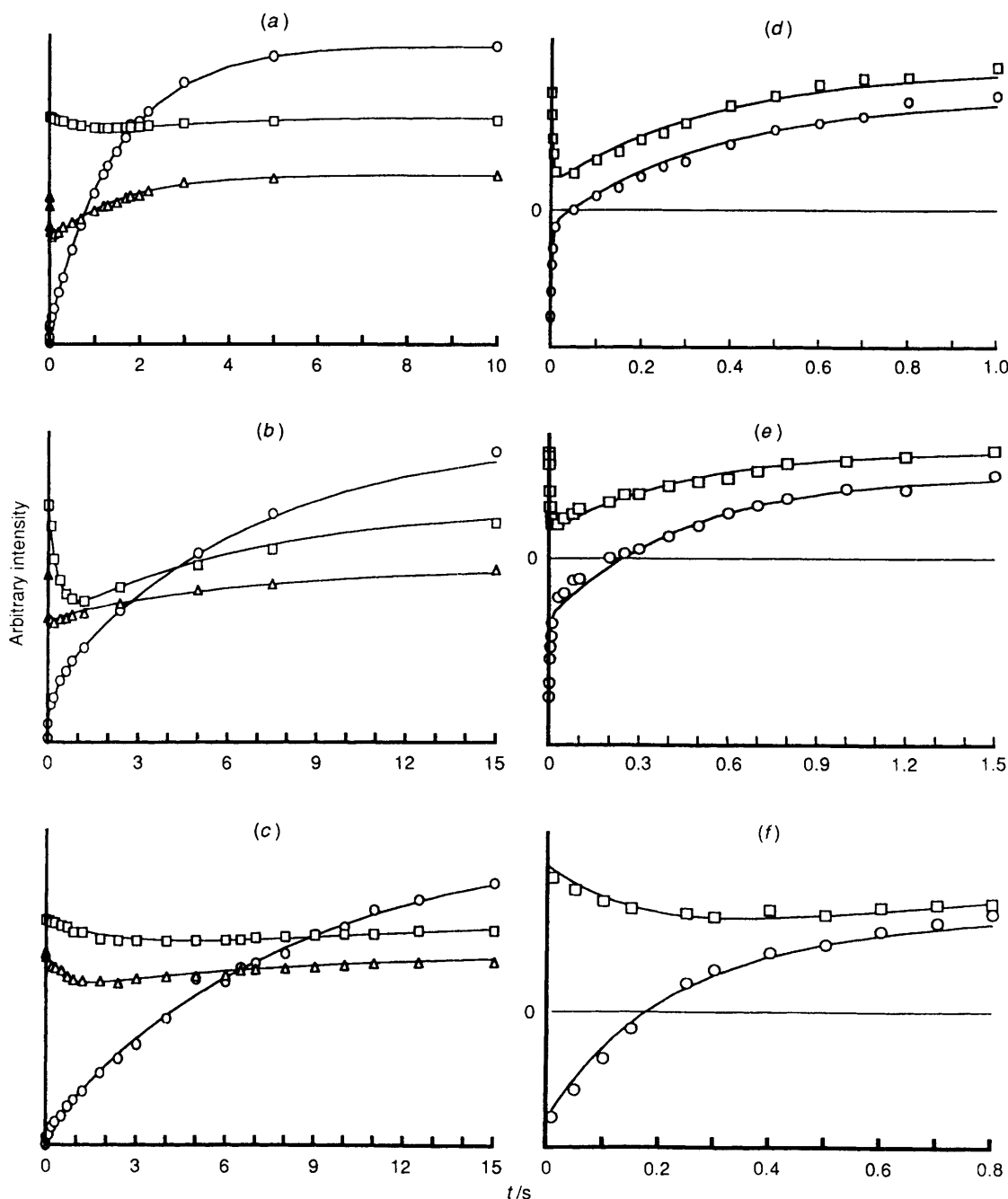


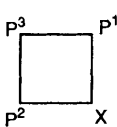
Fig. 4 (a)–(c) The dissociation of triphenylphosphines P_a and P_b in complexes **2a–2c** respectively as monitored by magnetisation transfer. (○), Experimental intensities of the inverted free phosphine; (□), intensities of the slow transfer to P_a ; (△), intensities of the fast transfer to P_b . The full curves represent the best fit by the kinetic models [equation (2)]. The intensities of the co-ordinated phosphines have been multiplied by 3 for clarity. (d)–(f) The isomerisation of H_a/H_b as monitored by the magnetisation transfer for **2a–2c** respectively. (○), Experimental intensities of the inverted hydride peak; (□), intensities of the transfer to the other peak. Full curves represent the best fit by the kinetic models [equation (6)]

Table 5 Unconstrained bond lengths (Å) and selected bond angles (°) for $[Rh(NH_3)(PPh_3)_3]ClO_4 \cdot MeOH$

Rh–P(1)	2.340(5)	Rh–P(3)	2.239(4)
Rh–P(2)	2.317(5)	Rh–N	2.14(1)
P(1)–C(1)	1.81(2)	P(2)–C(19)	1.85(2)
P(1)–C(7)	1.83(2)	P(2)–C(25)	1.85(2)
P(1)–C(13)	1.88(2)	P(2)–C(31)	1.84(2)
P(3)–C(37)	1.85(2)	P(3)–C(49)	1.82(2)
P(3)–C(43)	1.85(2)		
P(1)–Rh–P(2)	170.3(2)	P(2)–Rh–P(3)	94.3(2)
P(1)–Rh–P(3)	94.0(2)	P(2)–Rh–N	87.7(4)
P(1)–Rh–N	84.7(4)	P(3)–Rh–N	173.3(4)

presence of an equimolar concentration of $^{15}NO_3$ -enriched (*ca.* 24%) NBu_4NO_3 . Using a 20.26 MHz ^{15}N probe, there is *no* coalescence of these two resonances even at the boiling point of the solvent, CH_2Cl_2 . From line-broadening measurements it can be estimated that $k_{diss}(ONO_2)$ in **2b** at 298 K is *ca.* $45 s^{-1}$ which is very much lower than that found for **1b**, as expected due to the higher oxidation state, but is of similar magnitude to $k_{diss}(P_b)$ in **2b**. The mechanism for k_{diss} in all systems is probably dissociative and the difference in reaction rates between P_b and P_a phosphines simply reflects the difference in strength of the *trans* influence between the H and PPh_3 ligands.

Further support for this idea comes from the rate of hydride isomerisation, which in all systems is equal, within experimental error, to the dissociation rate of the equatorial

Table 6 Comparison of selected rhodium–phosphorus bond distances in related square-planar rhodium(I) complexes $[\text{RhX}(\text{PPh}_3)_3]$ ($\text{X} = \text{Cl}^2$ or ONO_2^8) and $[\text{RhX}(\text{PPh}_3)_3]\text{Y}$ ($\text{X} = \text{MeCN}$, $\text{Y} = \text{BF}_4^-$; $^{33} \text{X} = \text{NH}_3$, $\text{Y} = \text{ClO}_4^-$) and values of $^1J(\text{Rh}-\text{P})$


X = Cl						ONO ₂		MeCN		NH ₃	
	d/Å					d/Å	¹ J(Rh-P) ⁸ /Hz	d/Å	¹ J(Rh-P) ³³ /Hz	d/Å	¹ J(Rh-P)/Hz
Bond	Orange	Red	Red	Average	¹ J(Rh-P)/Hz						
Rh–P(1)	2.304(4)	2.322(4)	2.315(8)			2.307(3)		2.367(3)		2.340(5)	
Rh–P(2)	2.338(4)	2.334(4)	2.327(8)			2.351(3)		2.311(3)		2.317(5)	
Rh–P(3)	2.225(4)	2.214(4)	2.218(8)	2.219	189	2.212(3)	187	2.261(3)	170	2.239(4)	168
Rh–P(1,2)	2.321(4)	2.328(4)	2.321(8)	2.323	142	2.329(3)	148	2.339(3)	136	2.328(5)	142

Table 7 Rate constants for triphenylphosphine (P_a and P_b) dissociation and hydride isomerisation for octahedral $[\text{RhXH}_2(\text{PPh}_3)_3]^{n+}$ ($n = 0$, $\text{X} = \text{Cl}$ or ONO_2 ; $n = 1$, $\text{X} = \text{NH}_3$)

X	T/K	$k_{\text{diss}}(\text{P}_a)^a/\text{s}^{-1}$	$k_{\text{diss}}(\text{P}_b)^a/\text{s}^{-1}$	$k_{\text{iso}}^b/\text{s}^{-1}$
Cl	297	0.6	74	113
ONO ₂	303	2.5	96	120
NH ₃	303	≤0.1	2.1	2.3

^a k_{diss} is the rate of dissociation. ^b k_{iso} is the rate of isomerisation of H_a/H_b .

phosphine P_b , as can be seen in Table 7 and Fig. 4(d)–(f). Hence the mechanism of exchange probably proceeds *via* a five-coordinate trigonal-bipyramidal intermediate **6**, as previously suggested by Brown and co-workers^{7,25} rather than *via* the alternative trigonal twist mechanism found for $[\text{Ru}(\text{CO})\text{H}_2(\text{PPh}_3)_3]$ and recently suggested as being possible for the rhodium analogue **2a**.³⁴

Further insight into the mechanisms of isomerisation and ligand substitution in the square-planar rhodium(I) and octahedral rhodium(III) complexes could be gained by variation of solvent and temperature. However, the major problem to overcome is to reduce the experimental errors, which mainly arise because of the necessity to compromise between a reasonable time of measurement and the stability of the complexes *versus* good signal-to-noise ratios in the spectra.

The main dynamic effect observed in this work is that substitution of chloride in the $[\text{RhCl}(\text{PPh}_3)_3]$ complex with a labile and good leaving ligand like nitrate produces the biggest overall change in the rate constant for phosphine dissociation. However, it should be noted that hydrogen addition to the T-shaped molecule $[\text{Rh}(\text{PPh}_3)_3]^+$ does not occur³² in weakly co-ordinating solvents (e.g. CH_2Cl_2) and it seems necessary to have a ligand occupying the fourth site, albeit only weakly (e.g. tetrahydrofuran), before oxidative addition of hydrogen can occur to give the hydrogenation catalyst.

It thus seems unlikely that the formation of $[\text{Rh}(\text{PPh}_3)_3]^+$ from the rapid dissociation of ONO_2 in complex **1b** could be responsible for any increase in catalytic hydrogenation activity in non-polar solvents and further studies are underway to determine the relative catalytic hydrogenation activities of **1a**, **1b** and **1c**.

Acknowledgements

We thank, for financial support, Hovione S.A. (to J. R. and C. J.), the SERC (to G. L. M.) and Kungliga Fysiografiska

Sällskapet i Lund (to L. A. B.). We also thank Dr. P. R. Page (Hovione) for useful discussions.

References

- J. A. Osborn, F. H. Jardine, J. F. Young and G. Wilkinson, *J. Chem. Soc. A*, 1966, 1711.
- F. H. Jardine, *Prog. Inorg. Chem.*, 1981, **28**, 63.
- J. Halpern, *Inorg. Chim. Acta*, 1981, **50**, 11.
- D. Brown, B. T. Heaton and J. A. Iggo, in *Metal Promoted Selectivity in Organic Synthesis*, ed. A. F. Noels, Kluwer, Dordrecht, 1991, p. 329 and refs. therein.
- C. R. Bowers and D. P. Weitekamp, *J. Am. Chem. Soc.*, 1987, **109**, 5541.
- R. U. Kirss and R. Eisenberg, *J. Organomet. Chem.*, 1989, **359**, C22; R. Eisenberg, *Acc. Chem. Res.*, 1991, **24**, 110.
- J. M. Brown, P. L. Evans and A. R. Lucy, *J. Chem. Soc., Perkin Trans. 2*, 1987, 1589.
- B. T. Heaton, J. A. Iggo, C. Jacob, H. Blanchard, M. B. Hursthouse, I. Ghatak, M. E. Harman, W. Heggie, R. G. Somerville, P. R. Page and I. Villax, *J. Chem. Soc., Dalton Trans.*, 1992, 2533.
- P. Meakin, J. P. Jesson and C. A. Tolman, *J. Am. Chem. Soc.*, 1972, **94**, 3240.
- G. A. Morris and R. Freeman, *J. Magn. Reson.*, 1978, **29**, 433.
- B. E. Mann, *Spectrosc. Prop. Inorg. Organomet. Compd.*, 1985, **18**, 397.
- J. K. M. Sanders and B. K. Hunter, *Modern NMR Spectroscopy*, Oxford University Press, Oxford, 1987, p. 224.
- F. W. Dahlquist, K. J. Longmuir and R. B. Du Vernet, *J. Magn. Reson.*, 1975, **17**, 406.
- M. Grassi, B. E. Mann, B. T. Pickup and C. M. Spencer, *J. Magn. Reson.*, 1986, **69**, 92.
- H. M. McConnell, *J. Chem. Phys.*, 1958, **28**, 430.
- J. J. Led and H. Gesmar, *J. Magn. Reson.*, 1982, **49**, 444.
- M. Rudin, *Magn. Reson. Med. Biol.*, 1989, **2**, 177.
- G. A. Morris, personal communication.
- R. N. Stabler and J. Chesick, *Int. J. Kinet.*, 1978, **10**, 461.
- R. J. McKinney and F. J. Weigert, *Quantum Chemistry Program Exchange*, GEAR iterator, 1964, **11**, 22.
- F. J. Weigert, *Comput. Chem.*, 1987, **11**, 273.
- N. Walker and D. Stuart, *Acta Crystallogr., Sect. A*, 1983, **39**, 158.
- G. M. Sheldrick, program for crystal structure solution, SHELX 86, University of Göttingen, 1986.
- J. Halpern and C. S. Wong, *J. Chem. Soc., Chem. Commun.*, 1973, 629.
- J. M. Brown and A. R. Lucy, *J. Chem. Soc., Chem. Commun.*, 1984, 914.
- C. H. Langford and H. B. Gray, *Ligand Substitution Processes*, W. A. Benjamin, London, 1966, p. 33.
- J. M. Brown, P. A. Chaloner and G. A. Morris, *J. Chem. Soc., Chem. Commun.*, 1983, 664.
- J. M. Brown, P. A. Chaloner and G. A. Morris, *J. Chem. Soc., Perkin Trans. 2*, 1987, 1583.
- J. Burgess and P. Moore, in *Mechanisms of Inorganic and Organometallic Reaction*, ed. M. V. Twigg, Plenum, New York, 1983, vol. 1, p. 103.

- 30 R. J. Cross, in *Mechanisms of Inorganic and Organometallic Reactions*, ed. M. V. Twigg, Plenum, New York 1986, vol. 4, p. 161.
- 31 J. Burgess, in *Mechanisms of Inorganic and Organometallic Reactions*, ed. M. V. Twigg, Plenum, New York, 1989, vol. 6, p. 195.
- 32 A. R. Siedle, R. A. Newmark and R. D. Howells, *Inorg. Chem.*, 1988, **27**, 2473; Y. W. Yared, S. L. Miles, R. Bau and C. A. Reed, *J. Am. Chem. Soc.*, 1977, **99**, 7076.
- 33 G. Pimblett, C. D. Garner and W. Clegg, *J. Chem. Soc., Dalton Trans.*, 1985, 1977.
- 34 G. E. Ball and B. E. Mann, *J. Chem. Soc., Chem. Commun.*, 1992, 561.

Received 10th January 1994; Paper 4/00123K